Piippo, A., Salomäki, J., and Luomi, J. (2007). Signal injection in sensorless PMSM drives equipped with inverter output filter. In Proceedings of the Fourth Power Conversion Conference (PCC 2007), Nagoya, Japan, pp. 1105-1110.

Signal Injection in Sensorless PMSM Drives Equipped With Inverter Output Filter

Antti Piippo, Janne Salomäki, and Jorma Luomi
Power Electronics Laboratory
Helsinki University of Technology
P.O. Box 3000, FI-02015 TKK, Finland

***Abstract*— The paper proposes a hybrid observer for sensorless control of permanent magnet synchronous motor drives equipped with an inverter output LC filter. An adaptive full-order observer is augmented with a high-frequency signal injection method at low speeds. The only measured quantities are the inverter phase currents and the dc-link voltage. It is shown that the LC filter is not an obstacle to using signal injection methods. The proposed method allows sensorless operation in a wide speed range down to zero speed. Experimental results are given to confirm the effectiveness of the proposed method.**

***Index Terms*— Inverter output filter, permanent magnet motors, sensorless control, signal injection.**

I. Introduction

Problems may be encountered in ac motor drives due to the non-sinusoidal voltage produced by a pulse-width modulated (PWM) inverter. The high rate of change of the voltage (i.e. high $\mathrm{d}u/\mathrm{d}t$) may cause excessive voltage stresses in the stator winding insulations. It may also cause leakage currents through the parasitic capacitances of the stator winding and produce bearing currents. Voltage harmonics cause acoustic noise and power losses; the losses caused by eddy currents are a special concern in high-speed solid-rotor motors.

A common approach to overcome these problems is to use an inverter output filter [1]–[4]. An LC filter, having the resonance frequency below the switching frequency, is a typical choice for the filter topology if a nearly sinusoidal output voltage is required. However, this kind of heavy filtering makes the motor control more difficult. A conventional scalar control method is usually employed, but when better control performance is needed, a vector control method must be used. For vector control, the filter dynamics should be taken into account.

Various methods have been proposed for the vector control of variable-speed drives equipped with an LC filter. Methods based on feedforward action and sliding mode control have been used for compensating the effects of the filter in a sensorless permanent magnet synchronous motor (PMSM) drive in [2]. Direct measurement of the stator voltages and currents has been used for obtaining feedback signals for the current control and the speed and position estimation in a sensorless PMSM drive [3]. A feedforward current controller has been used in a speed-sensored synchronous reluctance motor drive with an LC filter [4]. For induction motor drives equipped with an LC filter, vector control methods based on cascaded controllers have been proposed in [5], [6].

Due to the LC filter, the voltages and currents at the motor terminals differ from those of the inverter output. Frequency converters are equipped with measurements of output currents, and output voltages are also known. For vector control, however, the corresponding quantities at the motor terminals are needed. In [2]–[6], the motor voltages or currents are measured by additional sensors, requiring hardware modifications in the motor drive. If the motor quantities are estimated instead, as in [7]–[9] for induction motor drives, the additional measurements are avoided and a filter can be added to an existing drive. Recently, a similar method has been proposed for sensorless PMSM drives [10].

The above mentioned sensorless techniques are based on fundamental-excitation methods, which do not allow sustained operation at low speeds. As a solution to this problem, high-frequency (HF) signal injection methods have been developed for sensorless PMSM drives without a filter [11]–[13]. However, such methods have not been previously applied to ac motor drives equipped with an inverter output LC filter.

In this paper, a hybrid observer is proposed where a speed-adaptive full-order observer [10] is augmented with a pulsating high-frequency (HF) signal injection technique [14] at low speeds. Signal injection methods are shown to be feasible even with the filter if the frequency of the injected voltage signal is suitably chosen. The proposed system is validated by means of simulations and laboratory experiments.

II. Filter and Motor Models

Fig. 1 shows a PMSM drive system equipped with an LC filter. The inverter output voltage $\mathbf{u}_A$ is filtered by the LC filter, resulting in a nearly sinusoidal stator voltage $\mathbf{u}_s$. The inverter output current $\mathbf{i}_A$ and the dc-link voltage u_{dc} are the only measured quantities.

The PMSM and the LC filter are modeled in the d-q reference frame fixed to the rotor. The d axis is oriented along the permanent magnet flux, whose angle in the stator reference frame is θ_m in electrical radians. The stator voltage equation is

$$\mathbf{u}_s = R_s\mathbf{i}_s + \dot{\boldsymbol{\psi}}_s + \omega_m\mathbf{J}\boldsymbol{\psi}_s \tag{1}$$

This work was financially supported by ABB Oy and Walter Ahlström foundation.

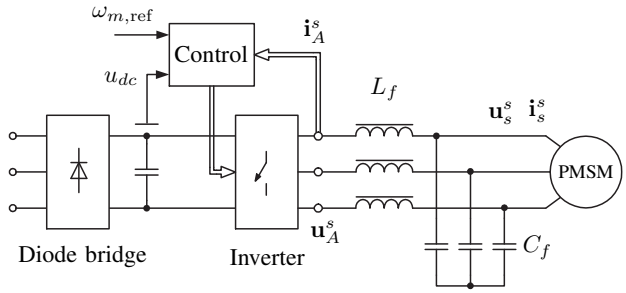

Fig. 1. PMSM drive system equipped with three-phase LC filter. Superscript s denotes the stator reference frame.

where $\mathbf{u}_s = [\,u_{sd} \quad u_{sq}\,]^T$ is the stator voltage, $\mathbf{i}_s = [\,i_{sd} \quad i_{sq}\,]^T$ the stator current, $\boldsymbol{\psi}_s = [\,\psi_{sd} \quad \psi_{sq}\,]^T$ the stator flux, R_s the stator resistance, $\omega_m = \dot{\theta}_m$ the electrical angular speed of the rotor, and

$$\mathbf{J} = \begin{bmatrix} 0 & -1 \\ 1 & 0 \end{bmatrix}$$

The stator flux is

$$\boldsymbol{\psi}_s = \mathbf{L}_s \mathbf{i}_s + \boldsymbol{\psi}_{pm} \tag{2}$$

where $\boldsymbol{\psi}_{pm} = [\,\psi_{pm} \quad 0\,]^T$ is the permanent magnet flux and

$$\mathbf{L}_s = \begin{bmatrix} L_d & 0 \\ 0 & L_q \end{bmatrix}$$

is the inductance matrix, L_d and L_q being the direct- and quadrature-axis inductances, respectively. The electromagnetic torque is given by

$$T_e = \frac{3p}{2} \boldsymbol{\psi}_s^T \mathbf{J}^T \mathbf{i}_s \tag{3}$$

where p is the number of pole pairs.

The LC filter equations are

$$\mathbf{u}_A - \mathbf{u}_s = R_{Lf} \mathbf{i}_A + L_f \dot{\mathbf{i}}_A + \omega_m L_f \mathbf{J} \mathbf{i}_A \tag{4}$$

$$\mathbf{i}_A - \mathbf{i}_s = C_f \dot{\mathbf{u}}_s + \omega_m C_f \mathbf{J} \mathbf{u}_s \tag{5}$$

where $\mathbf{i}_A = \begin{bmatrix} i_{Ad} & i_{Aq} \end{bmatrix}^T$ is the inverter current, $\mathbf{u}_A = \begin{bmatrix} u_{Ad} & u_{Aq} \end{bmatrix}^T$ the inverter output voltage, L_f the inductance and R_{Lf} the series resistance of the filter inductor, and C_f is the filter capacitance.

III. Control System

Fig. 2 shows a simplified block diagram of the control system (the estimated quantities being marked by the symbol $\hat{}$). The cascade control and speed-adaptive full-order observer are implemented in the estimated rotor reference frame. The estimated rotor position $\hat{\theta}_m$ is obtained by integrating $\hat{\omega}_m$. The inverter current, the stator voltage, and the stator current are controlled by PI controllers, and cross-couplings due to the rotating reference frame are compensated [5]. A maximum torque per current method is used for calculating the stator current reference [15]. The rotor speed is governed by a PI controller with active damping.

IV. Observer Structure

In the following, the speed-adaptive full-order observer proposed in [10] is augmented with an HF signal injection technique to stabilize the observer at low speeds. The two methods are combined in a fashion similar to [16]. The observer gain is modified for better compatibility with the HF signal injection method.

A. High-Frequency Signal Injection

The HF signal injection method is based on [14]. A carrier excitation signal

$$\mathbf{u}_c = \hat{u}_c \cos(\omega_c t) \begin{bmatrix} 1 \\ 0 \end{bmatrix}, \tag{6}$$

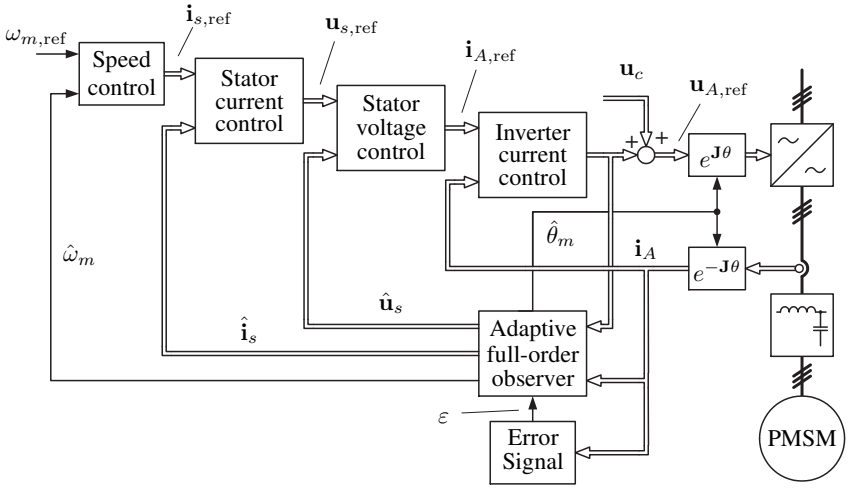

Fig. 2. Simplified block diagram of the control system. Double lines indicate vector quantities whereas single lines indicate scalar quantities. Vector quantities on the left-hand side of coordinate transformations are in the estimated rotor reference frame and on the right-hand side in the stator reference frame. The speed control includes the calculation of the stator current reference according to the maximum torque per current method.

TABLE I

SYSTEM DATA

Motor Data	
Nominal voltage U_N	370 V
Nominal current I_N	4.3 A
Nominal frequency f_N	75 Hz
Nominal torque T_N	14.0 Nm
Stator resistance R_s	3.59 Ω
Direct-axis inductance L_d	0.036 H
Quadrature-axis inductance L_q	0.051 H
Permanent magnet flux ψ_{pm}	0.545 Vs
Total moment of inertia	0.015 kgm^2
LC Filter Parameters	
Inductance L_f	5.1 mH
Capacitance C_f	6.8 μF
Series resistance R_{Lf}	0.1 Ω
Control System Parameters	
Inverter current control bandwidth	$2\pi\cdot600$ rad/s
Stator voltage control bandwidth	$2\pi\cdot400$ rad/s
Stator current control bandwidth	$2\pi\cdot200$ rad/s
Speed control bandwidth	$2\pi\cdot5$ rad/s
Speed adaptation bandwidth α_{fo}	$2\pi\cdot100$ rad/s
Bandwidth α_i at zero speed	$2\pi\cdot5$ rad/s

having amplitude $\hat{u}_c$ and angular frequency ω_c, is superimposed on the inverter voltage reference in the estimated rotor reference frame. An HF current response is detected on the q axis of the estimated rotor reference frame, amplitude modulated by the rotor position estimation error. The current signal is band-pass filtered, demodulated, and low-pass filtered to obtain an error signal, which is approximately

$$\varepsilon \approx K_\varepsilon \sin(2\tilde{\theta}_m) \tag{7}$$

where K_ε is the signal injection gain and $\tilde{\theta}_m = \theta_m - \hat{\theta}_m$ is the estimation error of the rotor position. Without the inverter output LC filter, the signal injection gain would be

$$K_\varepsilon = \frac{\hat{u}_c}{\omega_c}\frac{L_q - L_d}{4L_qL_d} \tag{8}$$

The error signal ε is used as a correction in the adaptive full-order observer as will be described in the following subsection.

To illustrate the effect of the filter, frequency responses of the system were calculated numerically. Parameters given in Table I were used for this example. The inverter d-axis current response to the inverter d-axis voltage is shown in Fig. 3(a) for the rotor position estimation error $\tilde{\theta}_m = 10°$. The amplitude response has a notch at the parallel resonance frequency of the filter capacitor and the stator inductance, and a peak at the LC filter resonance frequency. Above the frequency $f \approx 500$ Hz, the LC filter amplifies the response as compared to the response obtained for the PMSM without the filter.

Fig. 3(b) shows the inverter q-axis current response to the inverter d-axis voltage for the rotor position estimation error $\tilde{\theta}_m = 10°$. This response is important for the pulsating HF signal injection method. Compared to Fig. 3(a), the parallel resonance of the filter capacitance and the d-axis inductance cannot be seen in the response, but the LC filter resonance peak is visible. At higher frequencies, the

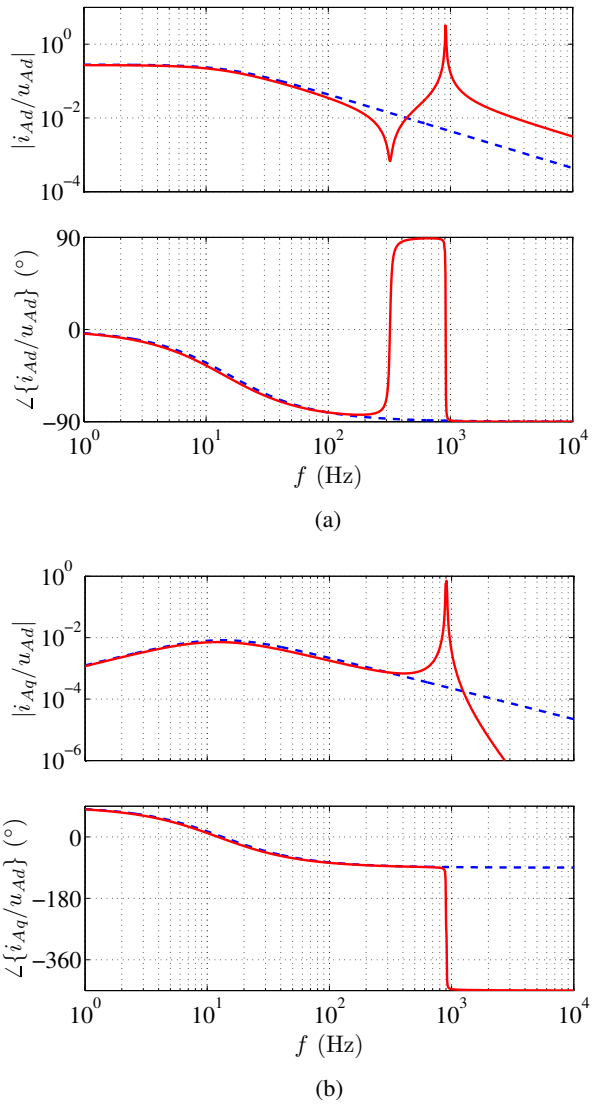

Fig. 3. Frequency responses of the system: (a) inverter d-axis current response to inverter d-axis voltage; (b) inverter q-axis current response to inverter d-axis voltage. Dashed lines show the response of the PMSM only, solid lines the response of LC filter and PMSM.

amplitude response decays rapidly. In HF signal injection, it is reasonable to select the frequency of the carrier excitation signal below the resonance frequency. If the excitation frequency is selected close to the resonance frequency, the HF current amplitude, and hence also the signal injection gain K_ε, are increased by the LC filter. At the frequency of 500 Hz, the LC filter increases the signal injection gain K_ε by a factor of 1.65 in this example.

B. Speed-Adaptive Full-Order Observer

The adaptive full-order observer is based on the dynamic models of the PMSM and the LC filter. The inverter current serves as the feedback signal for the observer, and the electrical angular speed of the rotor is estimated using an adaptation mechanism. The stator flux is selected as the state variable representing the electrical dynamics of the motor by inserting the stator current solved from (2) to

(1). When the dynamic equations of the filter are included, the observer is defined by

$$\dot{\hat{\mathbf{x}}} = \hat{\mathbf{A}}\,\hat{\mathbf{x}} + \hat{\mathbf{B}}\begin{bmatrix}\mathbf{u}_A & \hat{\boldsymbol{\psi}}_{pm}\end{bmatrix}^T + \mathbf{K}(\mathbf{i}_A - \hat{\mathbf{i}}_A) \tag{9}$$

where $\hat{\mathbf{x}} = \begin{bmatrix}\hat{\mathbf{i}}_A & \hat{\mathbf{u}}_s & \hat{\boldsymbol{\psi}}_s\end{bmatrix}^T$. The inverter voltage $\mathbf{u}_A$ and the permanent magnet flux estimate $\hat{\boldsymbol{\psi}}_{pm}$ are considered as inputs to the system. The system matrices and the observer gain matrix in (9) are

$$\hat{\mathbf{A}} = \begin{bmatrix} -\hat{R}_{Lf}\hat{L}_f^{-1}\mathbf{I} & -\hat{L}_f^{-1}\mathbf{I} & \mathbf{0} \\ \hat{C}_f^{-1}\mathbf{I} & \mathbf{0} & -\hat{C}_f^{-1}\hat{\mathbf{L}}_s^{-1} \\ \mathbf{0} & \mathbf{I} & -\hat{R}_s\hat{\mathbf{L}}_s^{-1} \end{bmatrix} - (\hat{\omega}_m - \omega_\varepsilon)\begin{bmatrix}\mathbf{J} & \mathbf{0} & \mathbf{0} \\ \mathbf{0} & \mathbf{J} & \mathbf{0} \\ \mathbf{0} & \mathbf{0} & \mathbf{J}\end{bmatrix} \tag{10}$$

$$\hat{\mathbf{B}} = \begin{bmatrix} \hat{L}_f^{-1}\mathbf{I} & \mathbf{0} \\ \mathbf{0} & \hat{C}_f^{-1}\hat{\mathbf{L}}_s^{-1} \\ \mathbf{0} & \hat{R}_s\hat{\mathbf{L}}_s^{-1} \end{bmatrix} \tag{11}$$

$$\mathbf{K} = \begin{bmatrix} k_{1d}\mathbf{I} + k_{1q}\mathbf{J} \\ k_{2d}\mathbf{I} + k_{2q}\mathbf{J} \\ k_{3d}\mathbf{I} + k_{3q}\mathbf{J} \end{bmatrix} \tag{12}$$

respectively, where $\mathbf{I}$ is the 2x2 unit matrix. The factors k_{id} and k_{iq} ($i = 1,\ 2,\ 3$) are scalar gain parameters. The estimate for the stator current, required for the controller feedback, is calculated based on (2):

$$\hat{\mathbf{i}}_s = \hat{\mathbf{L}}_s^{-1}(\hat{\boldsymbol{\psi}}_s - \hat{\boldsymbol{\psi}}_{pm}) \tag{13}$$

The speed adaptation law is

$$\hat{\omega}_m = -k_p\,(i_{Aq} - \hat{i}_{Aq}) - k_i \int (i_{Aq} - \hat{i}_{Aq})dt \tag{14}$$

where k_p and k_i are nonnegative adaptation gains. According to [16], these gains are selected as

$$k_p = \frac{2\alpha_{fo}}{\hat{\psi}_{pm}/\hat{L}_q}, \quad k_i = \frac{\alpha_{fo}^2}{\hat{\psi}_{pm}/\hat{L}_q} \tag{15}$$

where the design parameter α_{fo} corresponds to the approximate bandwidth of the speed adaptation.

In (10), the speed correction term ω_ε is based on the HF signal injection method. It is obtained from the error signal ε by means of a PI mechanism

$$\omega_\varepsilon = \gamma_p\varepsilon + \gamma_i \int \varepsilon dt \tag{16}$$

where γ_p and γ_i are nonnegative gains. The gains are selected as [17]

$$\gamma_p = \frac{\alpha_i}{2K_\varepsilon}, \quad \gamma_i = \frac{\alpha_i^2}{6K_\varepsilon} \tag{17}$$

where α_i is the approximate bandwidth of the PI mechanism. In (17), the influence of the LC filter on the signal injection gain K_ε should be taken into account.

The effect of the signal injection method is reduced linearly as the rotor speed increases, reaching zero at the transition speed ω_Δ. Both the HF excitation voltage $\hat{u}_c$ and the approximate bandwidth α_i of the PI mechanism in (16) are decreased, i.e.

$$\hat{u}_c = f(\hat{\omega}_m)\hat{u}_{c0}, \quad \alpha_i = f(\hat{\omega}_m)\alpha_{i0} \tag{18}$$

where $\hat{u}_{c0}$ and α_{i0} are the zero-speed values of the HF excitation voltage and the PI mechanism bandwidth, respectively. The function $f(\hat{\omega}_m)$ is shown in Fig. 4 as a function of the estimated rotor speed.

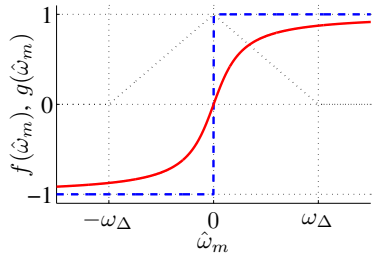

Fig. 4. Function $f(\hat{\omega}_m)$ (dotted), original function $g(\hat{\omega}_m)$ (dashed), and proposed function $g(\hat{\omega}_m)$ (solid) as functions of estimated rotor speed.

In [10], the observer gain was selected as

$$\mathbf{K} = \begin{bmatrix} k_{1d}\mathbf{I} \\ \mathbf{0} \\ k_{3d}\mathbf{I} + k_{3q}\underbrace{\operatorname{sign}(\hat{\omega}_m)}_{g(\hat{\omega}_m)}\mathbf{J} \end{bmatrix} \tag{19}$$

When the observer is augmented with the signal injection method, however, zero-speed operation becomes unstable due to the discontinuity of the signum function. It is better to use a smoother speed-dependent function

$$\mathbf{K} = \begin{bmatrix} k_{1d}\mathbf{I} \\ \mathbf{0} \\ k_{3d}\mathbf{I} + k_{3q}\underbrace{(2/\pi)\operatorname{atan}(k_s\hat{\omega}_m/\omega_\Delta)}_{g(\hat{\omega}_m)}\mathbf{J} \end{bmatrix} \tag{20}$$

where k_s defines the steepness of the $g(\hat{\omega}_m)$ function. A value $k_s = 5$ is used in the following. This modification is illustrated in Fig. 4.

V. Results

The proposed method was investigated by means of simulations and laboratory experiments. The data of the six-pole interior-magnet PMSM (2.2 kW, 1500 rpm) and the LC filter, and the cascade control bandwidths are given in Table I. The base values for the voltage, current, and angular speed are defined as $U_B = \sqrt{2/3}U_N$, $I_B = \sqrt{2}I_N$, and $\omega_B = 2\pi f_N$, respectively. The electromagnetic torque is limited to 22 Nm, which is 1.57 times the nominal torque T_N. The high-frequency carrier excitation signal has a frequency of 500 Hz and an amplitude of 30 V. The transition speed $\omega_\Delta = 0.13$ p.u. The digital implementation of the adaptive full-order observer is based on a simple symmetric Euler method [18], [7].

The experimental setup is illustrated in Fig. 5. The PMSM is fed by a frequency converter that is controlled by a dSpace DS1103 PPC/DSP board. Mechanical load is

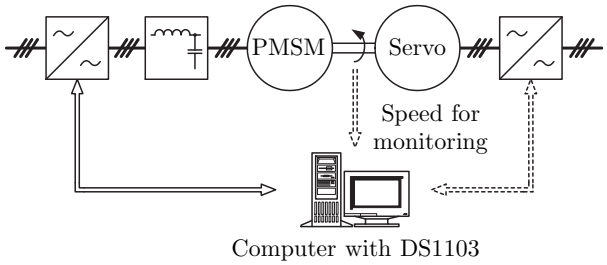

Fig. 5. Experimental setup. Mechanical load is provided by a servo drive.

provided by a PMSM servo drive. An incremental encoder is used for monitoring the actual rotor speed and position. The nominal dc-link voltage is 540 V, and the switching frequency and the sampling frequency are both 5 kHz. The dc-link voltage of the converter is measured, and simple current feedforward compensation is applied for dead times and power device voltage drops [19].

The MATLAB/Simulink environment was used for the simulations. The parameter values used in the controller were equal to those of the motor model. Simulation and experimental results showing speed reference steps at zero load torque are depicted in Fig. 6. The HF signal injection contributes to the rotor speed and position estimation at the speed ω_m = 0.05 p.u. The estimation accuracy for the rotor speed and position is good even at low speeds. The ripple in the measured results is caused by harmonics in the permanent magnet flux and in the motor inductances [20], and current measurement inaccuracies.

Fig. 7 shows simulation and experimental results at zero speed reference when nominal load torque steps are applied. The proposed observer is stable, both in transient and steady-state conditions. The rotor position estimation error stays small, indicating good dynamic properties. Experimental results showing a slow speed reversal at nominal load torque are depicted in Fig. 8. The system is stable both in the motoring and regenerating modes of operation, and sustained operation at low speeds is possible.

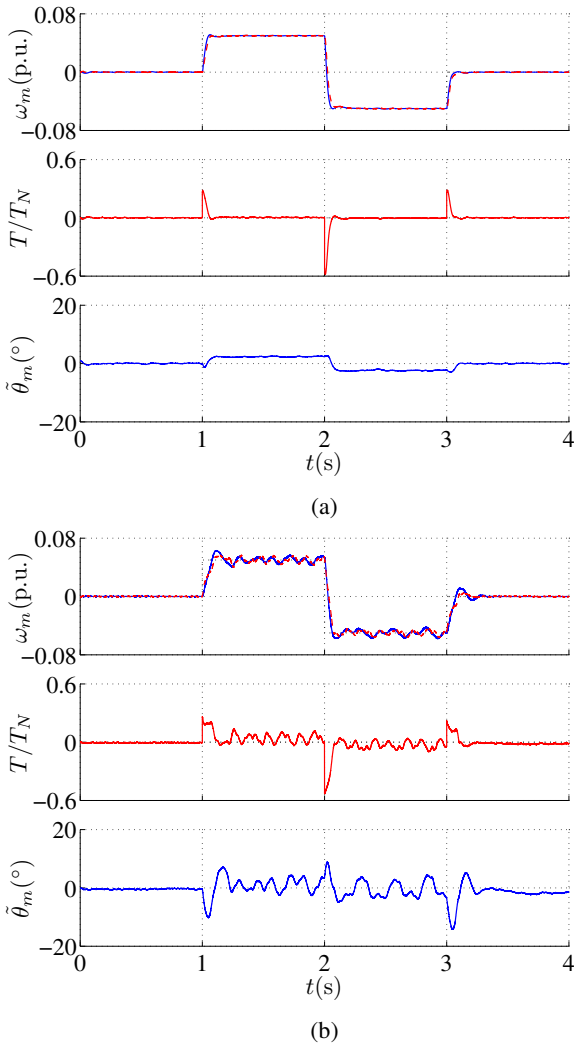

Fig. 6. Speed reference steps at no load: (a) simulation results; (b) experimental results. First subplot shows electrical angular speed (solid), its estimate (dashed), and its reference (dotted). Second subplot shows estimated electromagnetic torque (solid) and load torque reference (dotted). Last subplot shows estimation error of rotor position in electrical degrees.

VI. Conclusions

It is possible to use a signal injection method for the rotor speed and position estimation of PMSM drives even if an inverter output LC filter is used. The signal injection method is used for augmenting an adaptive full-order observer at low speeds. The simulation and experimental results show that the proposed system can cope with stepwise changes in the speed reference and load torque. The performance of the proposed sensorless method is comparable to that of a PMSM drive without the LC filter.

References

[1] Y. Murai, T. Kubota, and Y. Kawase, "Leakage current reduction for a high-frequency carrier inverter feeding an induction motor," *IEEE Trans. Ind. Applicat.*, vol. 28, no. 4, pp. 858–863, July/Aug. 1992.

[2] M. Carpita, D. Colombo, A. Monti, and A. Fradilli, "Power converter filtering techniques design for very high speed drive systems," in *Proc. EPE'01*, Graz, Austria, Aug. 1991.

[3] T. D. Batzel and K. Y. Lee, "Electric propulsion with sensorless permanent magnet synchronous motor: implementation and performance," *IEEE Trans. Energy Conversion*, vol. 20, no. 3, pp. 575–583, Sep. 2005.

[4] J.-D. Park, C. Khalizadeh, and H. Hofmann, "Design and control of high-speed solid-rotor synchronous reluctance drive with three-phase LC filter," in *Conf. Rec. IEEE-IAS Annu. Meeting*, Hong Kong, China, Oct. 2005, pp. 715–722.

[5] W. Zimmermann, "Feldorientiert geregelter Umrichterantrieb mit sinusförmigen Maschinenspannungen," *etzArchiv*, vol. 10, no. 8, pp. 259–266, Aug. 1988.

[6] M. Kojima, K. Hirabayashi, Y. Kawabata, E. C. Ejiogu, and T. Kawabata, "Novel vector control system using deadbeat-controlled PWM inverter with output LC filter," *IEEE Trans. Ind. Applicat.*, vol. 40, no. 1, pp. 162–169, Jan./Feb. 2004.

[7] J. Salomäki and J. Luomi, "Vector control of an induction motor fed by a PWM inverter with output LC filter," *EPE Journal*, vol. 16, no. 1, pp. 37–43, 2006.

[8] J. Salomäki, M. Hinkkanen, and J. Luomi, "Sensorless vector control of an induction motor fed by a PWM inverter through an output LC filter," *Trans. IEEJ*, vol. 126-D, no. 4, pp. 430–437, Apr. 2006.

[9] ——, "Sensorless control of induction motor drives equipped with inverter output filter," *IEEE Trans. Ind. Electron.*, vol. 53, no. 4,

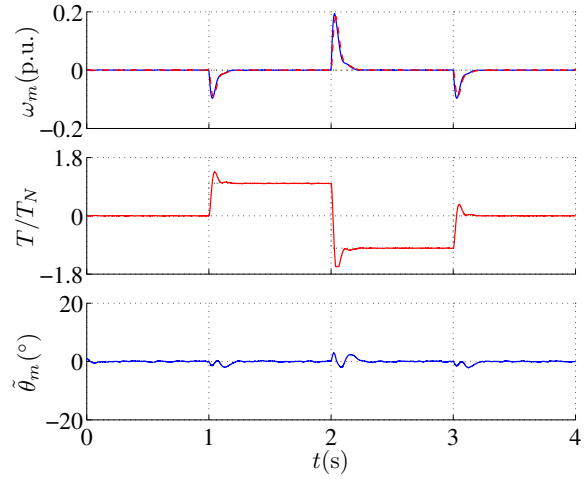

(a)

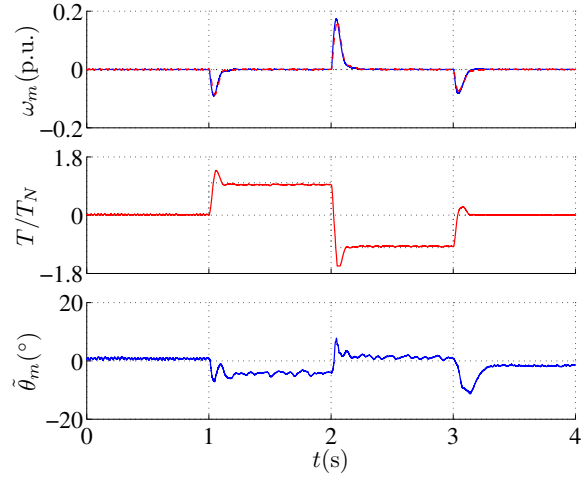

(b)

Fig. 7. Load torque steps at zero speed reference: (a) simulation results; (b) experimental results. Explanations of the curves are as in Fig. 6.

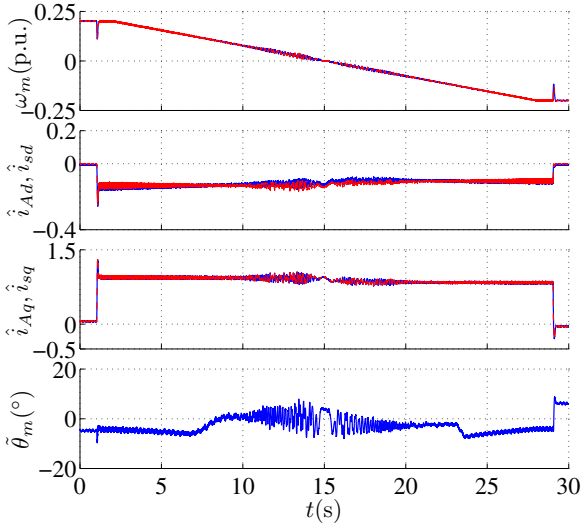

Fig. 8. Experimental results showing slow speed reversal at nominal load torque. First subplot shows electrical angular speed (solid), its estimate (dashed), and its reference (dotted). Second subplot shows estimated inverter d-axis current (solid) and estimated stator d-axis current (dotted), and third subplot corresponding q-axis currents. Last subplot shows estimation error of rotor position in electrical degrees.

Aug. 2006.

[10] J. Salomäki, A. Piippo, M. Hinkkanen, and J. Luomi, "Sensorless vector control of PMSM drives equipped with inverter output filter," in *Proc. IEEE IECON'06*, Paris, France, Nov. 2006, pp. 1059–1064.

[11] M. Schroedl, "Sensorless control of AC machines at low speed and standstill based on the INFORM method," in *Conf. Rec. IEEE-IAS Annu. Meeting*, vol. 1, San Diego, CA, Oct. 1996, pp. 270–277.

[12] P. L. Jansen and R. D. Lorenz, "Transducerless position and velocity estimation in induction and salient AC machines," *IEEE Trans. Ind. Applicat.*, vol. 31, no. 2, pp. 240–247, March/April 1995.

[13] M. Linke, R. Kennel, and J. Holtz, "Sensorless position control of permanent magnet synchronous machines without limitation at zero speed," in *Proc. IEEE IECON'02*, vol. 1, Sevilla, Spain, Nov. 2002, pp. 674–679.

[14] M. Corley and R. D. Lorenz, "Rotor position and velocity estimation for a salient-pole permanent magnet synchronous machine at standstill and high speeds," *IEEE Trans. Ind. Applicat.*, vol. 43, no. 4, pp. 784–789, July/Aug. 1998.

[15] T. Jahns, G. Kliman, and T. Neumann, "Interior permanent-magnet synchronous motors for adjustable-speed drives," *IEEE Trans. Ind. Applicat.*, vol. 22, no. 4, pp. 738–747, July/Aug. 1986.

[16] A. Piippo and J. Luomi, "Adaptive observer combined with HF signal injection for sensorless control of PMSM drives," in *Proc. IEEE IEMDC'05*, San Antonio, TX, May 2005, pp. 674–681.

[17] A. Piippo, M. Hinkkanen, and J. Luomi, "Sensorless control of PMSM drives using a combination of voltage model and HF signal injection," in *Conf. Rec. IEEE-IAS Annu. Meeting*, vol. 2, Seattle, WA, Oct. 2004, pp. 964–970.

[18] J. Niiranen, "Fast and accurate symmetric Euler algorithm for electromechanical simulations," in *Proc. Electrimacs'99*, vol. 1, Lisboa, Portugal, Sept. 1999, pp. 71–78.

[19] J. K. Pedersen, F. Blaabjerg, J. W. Jensen, and P. Thogersen, "An ideal PWM-VSI inverter with feedforward and feedback compensation," in *Proc. EPE'93*, vol. 5, Brighton, UK, Sept. 1993, pp. 501–507.

[20] A. Piippo and J. Luomi, "Inductance harmonics in permanent magnet synchronous motors and reduction of their effects in sensorless control," in *Proc. ICEM/2006*, no. 138, Chania, Greece, Sept. 2006, CD-ROM.